IOP Publishing New J. Phys. 28 (2026) 015001 https://doi.org/10.1088/1367-2630/ae2dfc

New Journal of Physics
The open access journal at the forefront of physics

Deutsche Physikalische Gesellschaft DPG
IOP Institute of Physics

Published in partnership with: Deutsche Physikalische Gesellschaft and the Institute of Physics

PAPER

Experimental investigation of stochastic resetting in a non-Markovian environment

Félix Ginot* and **Clemens Bechinger**

Fachbereich Physik, Universität Konstanz, 78457 Konstanz, Germany
* Author to whom any correspondence should be addressed.

E-mail: felix.ginot@uni-konstanz.de

Keywords: non-Markovian baths, stochastic resetting, colloidal particles

Supplementary material for this article is available online

OPEN ACCESS

RECEIVED
16 May 2025

REVISED
13 November 2025

ACCEPTED FOR PUBLICATION
8 December 2025

PUBLISHED
13 January 2026

Abstract

Stochastic resetting (SR), in which a system intermittently returns to a fixed location, is a powerful strategy for optimizing search processes. While extensively studied in memoryless (Markovian) systems, its behavior in complex media with memory remains largely unexplored. Here, we experimentally investigate SR in a viscoelastic fluid by tracking a colloidal particle subjected to intermittent resets. In this non-Markovian environment, the fluid's memory gives rise to elastic restoring forces that oppose the reset, pulling the particle back toward its prior position and hindering efficient exploration. We show that these memory effects can be actively controlled: by holding the particle at the trap center for a sufficient time, the fluid relaxes, erasing its memory and allowing the system to re-equilibrate. When introducing a fixed target site, we find that this memory control enables a significant reduction in the mean passage time, with optimal search performance emerging at intermediate resetting frequencies. In this regime, memory enhances performance through a 'bunching' effect, in which the particle rapidly revisits the target due to temporal correlations in its trajectory. These results highlight the dual role of memory in resetting dynamics-as both a hindrance and a resource-and suggest new strategies for optimizing search in non-Markovian systems, with potential applications in soft matter, biological transport, and stochastic control.

1. Introduction

Stochastic resetting (SR) is widely observed in nature as an efficient search strategy, from foraging animals that reinitialize their search areas for food to molecular motors which optimize the location of binding sites on DNA [1–4]. This process, in which a dynamical system intermittently returns to a predefined state, helps avoid inefficient sampling of the available space toward a specific target site [5–10]. In diffusive search processes, SR can drastically reduce first-passage times (FPTs) even when only minimal information about the system is available, making it a powerful tool for addressing search problems in both natural and algorithmic settings [5, 11–18]. It has also been applied in computational algorithms, particularly in optimization tasks, where resetting helps escape local optima and improves convergence to better solutions [19–21].

While recent theoretical studies have additionally explored the role of memory in SR [22–31], current experimental investigations have focused almost exclusively on Markovian systems, where memory is absent and all information about past trajectories is lost instantly [14, 32, 33]. However, under realistic conditions, often memory effects are present rendering non-Markovian dynamics strongly influencing the search dynamics [34–37]. Memory can both enhance performance, by biasing motion toward previously successful trajectories [38], and reduce it, by resisting resets and trapping the system in suboptimal states.

Here we experimentally investigate SR in a non-Markovian in a viscoelastic fluid, where time-delayed mechanical responses encode memory of past trajectories. We uncover a fundamental trade-off: fluid memory hinders resetting by pulling the particle back toward its pre-reset location, yet it also produces

correlated 'bunching' events where the particle rapidly re-encounters a target multiple times. Crucially, we demonstrate that this memory can be tuned experimentally by controlling the holding time after each reset. Short holding times preserve memory and favor rapid re-targeting, while longer ones allow relaxation and erasure of memory, enabling efficient exploration. By selectively managing memory in this way, we achieve up to a tenfold reduction in mean passage times (MPTs) compared to a memoryless system. Our results demonstrate that memory effects can strongly reduce MPTs which may opens new directions for optimizing search processes in biological, physical, and algorithmic systems that inherently operate in non-Markovian environments.

2. Experimental setup

We perform experiments using a silica particle with a diameter of 2.73 μm, freely diffusing at the surface of a capillary with a thickness of 100 μm, filled with a viscoelastic fluid (see below). Particle positions are recorded using a video camera operating at 100 Hz, with a spatial resolution of ± 6 nm. In the experiments we only consider positions on the x axis, which is positioned perpendicular to the capillary, in order to greatly reduce any drift originating from an imperfect sealing. An optical tweezer is generated by tightly focusing a 1064 nm laser beam through a 100x oil immersion objective. The beam passes through an acousto-optic modulator, allowing rapid control of the laser intensity. In the following, we use a two-state protocol. When the laser is on, the intensity is set to 0.3 W, generating a strong optical trap with stiffness $\kappa \sim 100\,\mu\mathrm{N\,m^{-1}}$ over a $\sim 5\,\mu$m area, which effectively suppresses thermal fluctuations and holds the particle fixed at $x = 0$. When the laser is off, the particle is free to diffuse.

The viscoelastic fluid used in the experiments consists of an equimolar solution (8 mM) of cetylpyridinium chloride monohydrate (CPyCl) and sodium salicylate (NaSal), which self-assemble into a dynamic network of giant wormlike micelles (WLMs) [39, 40]. The fluid's relaxation time, determined via recoil experiments [41, 42], is approximately $\tau_R \approx 6$ s. All experiments were conducted at a constant temperature of 25 °C. Further details on sample preparation and the experimental setup can be found in the supplementary materials (SM).

3. Resetting process

We first consider the case of a one-dimensional SR process, as illustrated in figure 1(a). Initially, the laser is switched off, and the particle, located at position $x(t)$, diffuses freely along the surface of the capillary. A resetting event is initiated by activating the optical tweezer, which rapidly pulls the particle back toward the origin at $x = 0$. Once the particle reaches the trap center, it is held in place for a duration t_h, after which the laser is turned off, completing the reset. The holding time can been varied between 0.1 s up to several seconds and thus covers the range below and above the fluid's relaxation time τ_R. The resetting process is repeated continuously, with the waiting time τ between consecutive resets drawn from an exponential distribution, $P(\tau) = \lambda e^{-\lambda\tau}$, where λ is the Poissonian resetting rate, commonly considered in SR studies [5]. In figure 1(b), we show a typical experimental trajectory segment (blue line), with red triangles indicating reset events. Over time, the system approaches a non-equilibrium steady state, characterized by a stationary probability density function $P(x)$ and a non-vanishing probability flux [5, 7, 43].

In figure 2(a), we show the spatial probability density function $P(x)$ for various resetting rates λ, using a holding time of $t_h = 0.1$ s. Importantly, these distributions exclude data recorded during the resetting phase-including the holding period t_h-during which the particle is actively pulled back to the origin. This exclusion avoids biasing the statistics and is consistent with prior studies showing that including such phases will significantly distort $P(x)$ [44]. By pruning the trajectory in this way, we effectively implement an idealized instantaneous resetting protocol, where the particle immediately moves from its pre-reset to post-reset position, as described in [33]. As expected, increasing λ results in more frequent resets, thereby confining the particle closer to the origin and leading to a narrower spatial distribution.

These experimental observations are supported by numerical simulations based on a minimal micromechanical model designed to capture the non-Markovian properties of the surrounding fluid. The model includes a fictitious 'bath' particle with friction coefficient γ_B, harmonically coupled to the colloidal particle (with friction γ_t) via a spring of stiffness κ_B (see SM). This coupling introduces a delayed stress response that effectively reproduces the viscoelastic behavior of the environment [41, 45]. Notably, the three model parameters have been independently determined in previous experiments. As shown in figure 2(b), the simulations qualitatively reproduce the experimental stationary distributions shown in

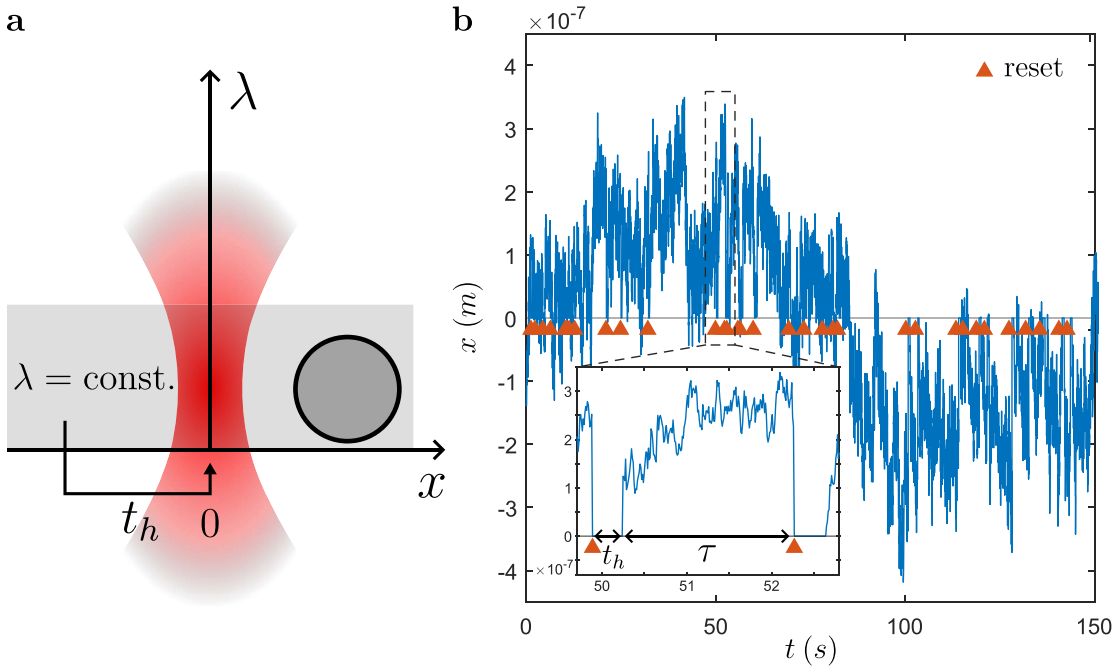

Figure 1. (a) Sketch of the resetting process. A particle is freely diffusing at the surface of the capillary and is stochastically reset to position $x = 0$, for a fixed rate $\lambda(x) = const.$ using a tight optical tweezer. The particle is held in place for a time t_h before being released. (b) Typical trajectory of a colloidal particle suspended in a viscoelastic bath and under the resetting process. Reset events (red triangles) are happening after a stochastic time τ, and last for a time t_h. The position of the particle was set to 0 during the resetting event for better visualization.

figure 2(a), accurately capturing their shape and the dependence of their width on λ. A closer agreement between experiments and simulations can be achieved by extending the model to include a second bath particle. As shown previously [41], this additional degree of freedom is required to fully capture the relaxation dynamics of the viscoelastic medium (see SM).

In the case of SR in memory-free environments such as Newtonian fluids, it has been established that a Poissonian SR produces a Laplace distribution for $P(x)$, featuring symmetric exponential tails [5]. This behavior is confirmed in our own Brownian dynamics simulations (figure 2(b), black line), which serve as a baseline for the memoryless case. In these simulations, the colloidal and bath particles are merged into an *effective* single particle with total friction $\gamma = \gamma_t + \gamma_B$ (see SM). Additional experimental measurements performed in water, which similarly yield Laplace-shaped distributions with exponential tails, are provided in the Supplementary Materials. Clearly, both experimental and simulated distributions in non-Markovian environments strongly depart from the Laplace form, exhibiting broader tails that deviate from the characteristic exponential decay. For instance, at a fixed resetting rate $\lambda = 0.2\,\mathrm{s}^{-1}$ and holding time $t_h = 0.1\,\mathrm{s}$, $P(x)$ in the viscoelastic fluid (light green line) is significantly broader than in the Newtonian fluid (black line). To achieve a similar width of $P(x)$ in the viscoelastic case, the resetting rate must be increased by an order of magnitude to $\lambda = 2\ \mathrm{s}^{-1}$ (dark blue line).

To assess how fluid memory affects SR, in the following we vary the holding time t_h-the period during which the particle is trapped at $x = 0$ after each reset. This time interval determines how much of the fluid's memory is retained before the particle is released: short (compared to τ_R) holding times preserve memory, while longer ones allow relaxation, effectively erasing strain information stored in the fluid [46]. We remind here that t_h was excluded from the trajectory during the analysis. In other words, the trivial effect of keeping the particle at $x = 0$ for a longer period is removed, allowing us to isolate and highlight the impact of t_h once the particle is released. Figure 2(c) shows experimental measurements of the steady-state probability density $P(x)$ for two representative values of t_h: 0.1 s and 5 s, with a fixed resetting rate $\lambda = 0.2\ \mathrm{s}^{-1}$. These values are below and near the fluid's relaxation time $\tau_R \approx 6$ s. For $t_h \ll \tau_R$, the fluid has insufficient time to relax, and memory of the particle's pre-reset motion persists, resulting in broad, memory-dominated distributions. In contrast, for $t_h \sim \tau_R$, memory effects diminish, and $P(x)$ becomes narrower, approaching the Laplace-like form expected in Markovian resetting [29]. This trend is mirrored in simulations (figure 2(d)), which qualitatively reproduce the dependence of $P(x)$ on t_h. These results confirm that the holding time acts as a tunable parameter that controls the degree

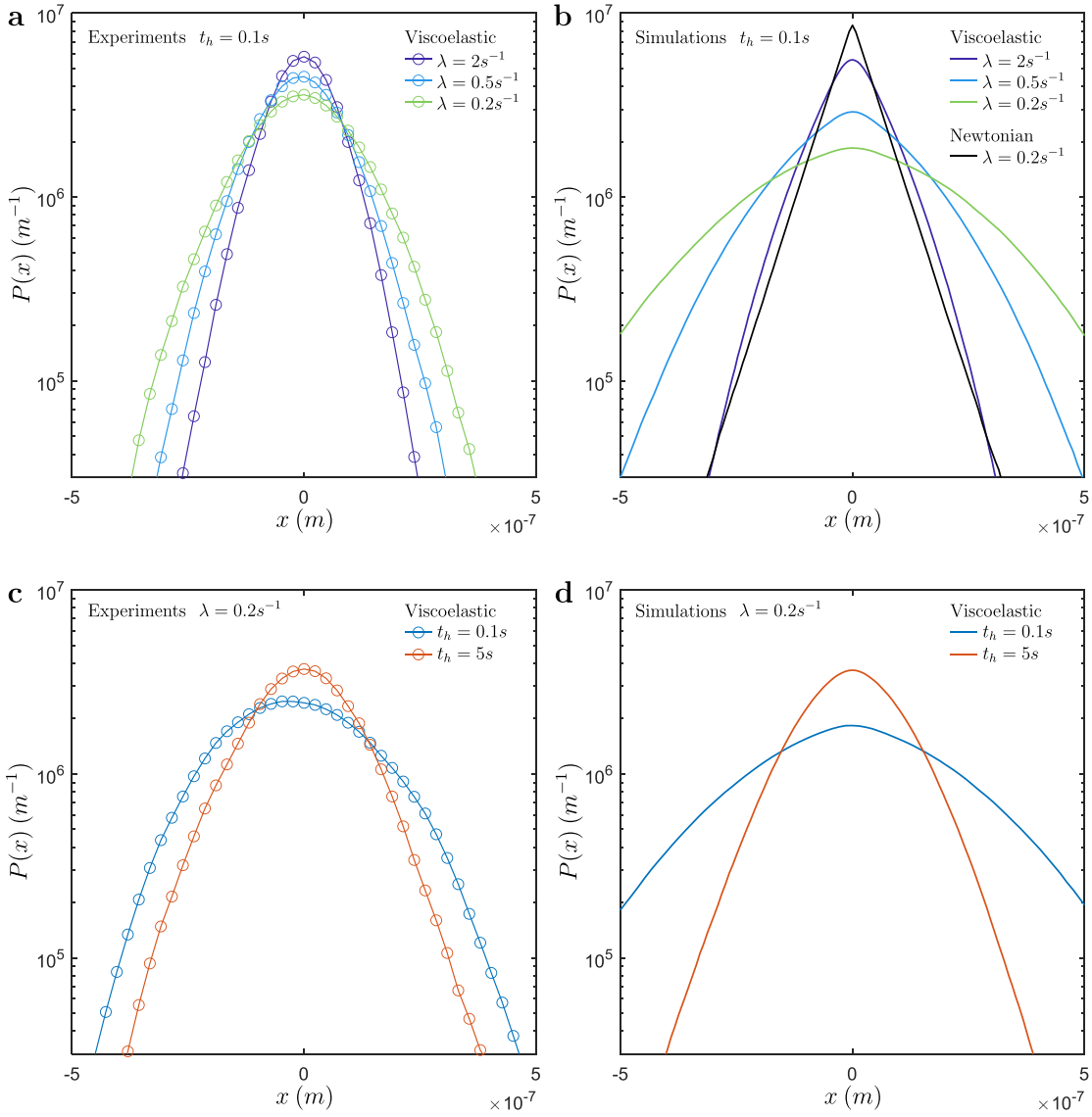

Figure 2. (a) Experimental (symbols with lines) probability density function $P(x)$ of finding the colloidal particle at a given position under a continuous resetting process, for a fixed value of $t_h = 0.1$ s and different resetting rates λ. (b) Simulated (lines) probability density function $P(x)$ under the same conditions, showing a qualitatively similar behavior to the experiments. In black we show the Laplace distribution obtained within a Newtonian (Markovian) environment. (c) Experimental (symbols with lines) probability density function $P(x)$ of finding the colloidal particle at a given position under a continuous resetting process, for a fixed value of $\lambda = 0.2\ s^{-1}$ and $t_h = 0.1$ s (blue) and $t_h = 5$ s (red). (d) Simulated (lines) probability density function $P(x)$ under the same conditions, showing a qualitatively similar behavior to the experiments.

of non-Markovianity in the system. Obviously, such sensitivity to t_h is absent in Newtonian fluids, which instantaneously relax compared to colloidal timescales.

The influence of fluid memory is also evident in the particle's dynamics following a reset. When t_h is short, the environment retains directional information, inducing a recoil motion that biases the particle toward its pre-reset position. This systematic drift introduces a transient deviation from purely diffusive motion and prevents the system from instantaneously reaching mechanical equilibrium. These effects are clearly visible in experimental trajectories: after each reset, the particle consistently moves toward its prior location (figure 1(b), inset). On longer timescales, this gives rise to persistent spatial correlations, as seen in figure 1(b), where the trajectory remains predominantly on one side of the origin-$x \gtrsim 0$ for $t < 80$ s and $x \lesssim 0$ thereafter-despite continuous resetting. Overall, these observations reveal how viscoelastic memory resists the resetting process, diminishing its confining effect and broadening the steady-state distribution. Crucially, this resistance can be modulated through t_h, providing an experimental handle to explore and harness memory effects in non-equilibrium transport.

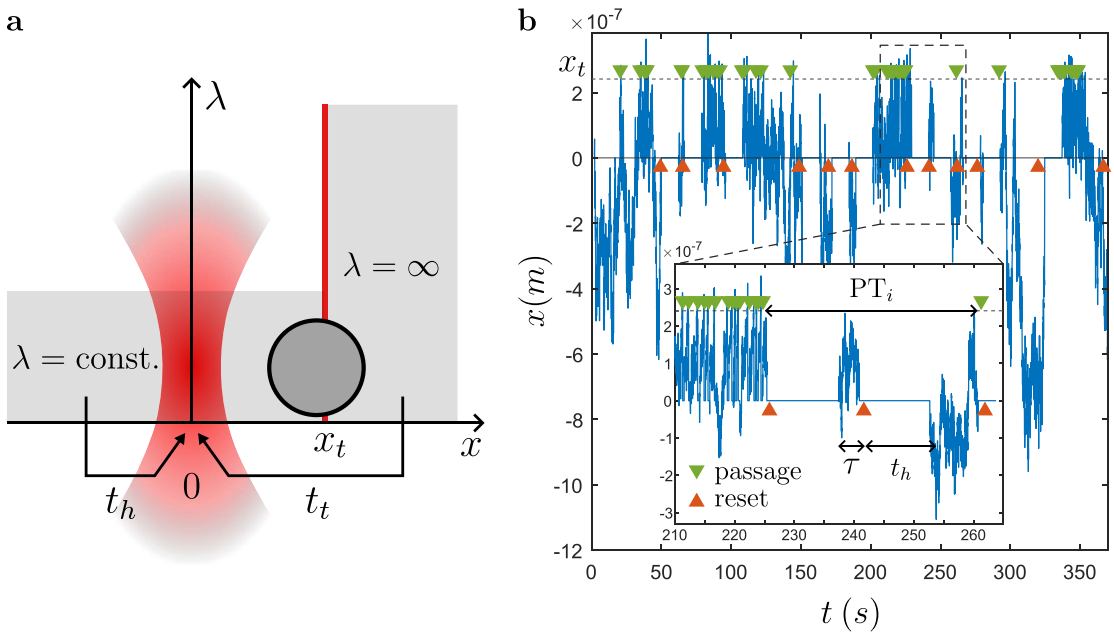

Figure 3. (a) Sketch of the resetting process with the addition of a target at position x_t: for $x > x_t$ we systematically reset the particle's position, and thus $\lambda = \infty$. (b) Typical trajectory of a colloidal particle suspended in a viscoelastic bath and under a resetting process, with a target at position x_t. Passage times (PT) are measured as the time between two passage events (green down triangles). Reset events (red up triangles) are happening after a stochastic time τ, and last for a time t_h during which the particle is held at position $x = 0$ with a strong optical tweezer.

4. Optimizing a search process

We now turn to the implications of memory during a simple search optimization problem using SR. The experimental protocol is schematically illustrated in figure 3(a). Each time the particle reaches a target at position x_t, we record a passage event i with corresponding PT PT_i, and apply a reset with a short holding time $t_t = 0.1$ s (note the index t instead of h). In addition to these target-triggered resets, we apply the above Poissonian SR with rate λ and varying holding time t_h which ensures to limit our experimental timescales by preventing excessively long excursions away from the target. It is important to emphasize that our setup implements a target-resetting protocol rather than an absorbing-boundary condition. In Markovian systems, these two formulations are equivalent because memory is lost instantaneously after each reset. In contrast, in our non-Markovian fluid, they differ fundamentally: the bath retains information about the particle's pre-reset motion. This distinction is crucial, as an absorbing-boundary approach would effectively erase this memory after every passage event, thereby eliminating the non-Markovian effects we seek to study. The distinction between complete and incomplete renewal processes in the context of SR has recently been discussed in detail in numerical studies [31]. More information regarding the PT statistics, is available in SM. A segment of a representative experimental trajectory is shown in figure 3(b), where the reset events triggered by target encounters are marked by green down triangles, while stochastic resets due to the Poisson process are indicated in red. Strikingly, the target-hitting events are not evenly spaced in time but are apparently correlated -a phenomenon we refer to as *bunching* in the following, and which will we analyze in more detail below. Unlike the FPT in memory-free systems which are fully uncorrelated between subsequent realizations, this is no longer true in a viscoelastic fluid where—depending on the value of t_h some memory of the past is retained. Therefore, in the following we will refer to PT instead of FPT. Additional numerical examples illustrating the discrepancy between PT and FPT statistics in Markovian and non-Markovian resetting are provided in the SM.

Figure 4(a) shows the MPT $= \langle PT_{i+1} \rangle_i$ as a function of the Poissonian reset rate λ for different values of t_h. As in memoryless systems [12, 14, 16], we observe a non-monotonic dependence: The MPT reaches a minimum at an intermediate λ, indicating an optimal balance between exploration and resetting. For large λ, exploration is limited by frequent resets which prevent the particle from reaching the target, while at low λ, the dynamics converges towards free diffusion, leading to long-tailed PT distributions and increased search times [12, 47]. The optimal search performance thus emerges at intermediate resetting rates, where exploration and reset are balanced.

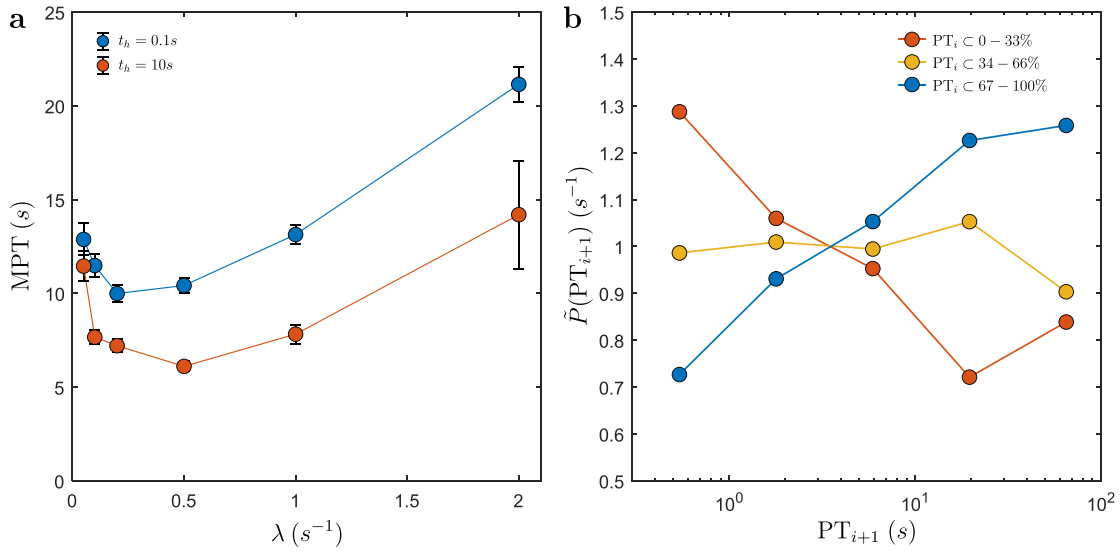

Figure 4. (a) Mean passage time (MPT) as a function of the resetting rates λ, for $t_\mathrm{h} = 0.1$ and 10 s (blue and red respectively). (b) Normalized probability of finding an event $\tilde{P}(\mathrm{PT}_{i+1})$ knowing that the previous event PT_i was either part of the fast (red), average (orange) or slow (blue) tertile.

To quantify the observed bunching, we analyze correlations between successive PTs. We first sort all recorded PTs in ascending order, from the fastest to the slowest, and partition them into three quantiles of equal size (tertiles). For each subset which contains events PT_i, we then compute the distribution of immediately following PTs PT_{i+1} and normalize it by the global PT distribution: $\tilde{P}(\mathrm{PT}_{i+1}) = P(\mathrm{PT}_{i+1}|\mathrm{PT}_i)/P(\mathrm{PT})$. This normalization allows to better differentiate distributions which span several orders of magnitudes and would therefor look very similar. The results, shown in figure 4(b), reveal strong temporal correlations. Fast events (lowest tertile, $\mathrm{PT}_i \subset 0-33\%$) are typically followed by another fast event, indicated by $\tilde{P}(\mathrm{PT}_{i+1} \lesssim 4\,\mathrm{s}) > 1$, and a corresponding depletion of slower events ($\tilde{P}(\mathrm{PT}_{i+1} \gtrsim 4\,\mathrm{s}) < 1$). Conversely, for the slowest tertile ($\mathrm{PT}_i \subset 67-100\%$), the opposite trend is observed. These findings show that in non-Markovian environments, incomplete resets not only broaden the steady-state spatial distribution, but also imprint memory into the sequence of events, enhancing the likelihood of temporally clustered target encounters. More information regarding the PT_i correlations, is available in SM.

However, while these correlations can facilitate rapid target re-encounters, they also come at a cost. As shown in figure 2, resets performed with short holding times (e.g. $t_\mathrm{h} = 0.1$ s) fail to fully erase the memory stored in the fluid's internal degrees of freedom, especially after long excursions. In such cases, residual restoring forces drive the particle back toward its previous position, regardless of whether this motion aids or hinders the search. As a result, memory not only reinforces returns to the target but also prolongs unproductive trajectories, ultimately broadening the passage-time distribution and reducing search efficiency. In this context, the holding time t_h emerges as a crucial control parameter. By tuning its duration, one can regulate the extent of memory retained after a reset. For example, keeping t_t short ($t_\mathrm{t} \ll 1$) after successful target encounters preserves advantageous passage-time correlations, while increasing t_h during stochastic resets allows the system to relax and erase detrimental memory effects. In this way, the strategy exploits fluid memory in a statistically biased manner, favoring rapid rediscovery after target encounters while mitigating its adverse influence during exploration. The benefit of this approach is demonstrated in figure 4(a). When the holding time for Poissonian resets is increased to $t_\mathrm{h} = 10$ s (red curve), the MPT drops by nearly 50% compared to the baseline case with $t_\mathrm{h} = 0.1$ s (blue curve). Additionally, the optimal resetting rate shifts toward lower values, consistent with the idea that both increasing t_h and decreasing λ narrow the steady-state distribution $P(x)$ and thereby enhance search efficiency. For clarity, the PT statistics reported here exclude the resetting intervals, thereby focusing solely on the effective dynamical gains produced by memory control. This approach highlights the intrinsic acceleration arising from optimized resetting, independent of the time spent on memory erasure. In our experiments, relaxation occurs passively (meaning the absolute gain is offset by a time penalty) but this represents a conservative limit: active control strategies-such as accelerating fluid relaxation through heating or other perturbations-could dramatically shorten the erasure phase. Such methods

would convert the demonstrated speedup into an absolute acceleration, offering a promising route for future experimental implementations.

Finally, we emphasize that our study does not address the thermodynamic aspects of resetting. Recent works [33, 48] have shown that resetting is akin to erasing positional information, a process that is intrinsically associated with a work cost. This cost increases not only with the resetting frequency but also with how fast the reset itself is applied. Accounting for this cost, and for the finite time required to perform the reset, introduces an additional and nontrivial trade-off between minimizing FPTs and minimizing energetic expenditure. In non-Markovian fluids, which carry an additional, persistent form of memory, erasure entails an extra thermodynamic cost. We therefore expect such trade-offs between performance and energetic cost to become even more pronounced in non-Markovian environments.

5. Summary and discussion

The resetting protocol explored in this study represents a minimal search strategy, with a basic control over memory effects. Specifically, we showed that the partial erasure of memory enhances the exploration efficiency of the particle by preventing it from recoiling toward its pre-reset position. However, due to the stochastic nature of Poissonian resetting, short inter-reset times τ can still occur unpredictably-even immediately after a successful target encounter. In such cases, a premature memory erasure may disrupt advantageous temporal correlations and hinder exploitation.

To address this, more refined resetting protocols could be implemented. For example, one might replace Poissonian resets with deterministic ones that occur only after a minimum time has elapsed, reducing the likelihood of memory loss during critical exploitation phases. Alternatively, adaptive schemes could be envisioned, in which the holding time t_{h} is dynamically modulated based on the preceding τ, or conditioned on the detection of successful target encounters. Such strategies would enable better control over the balance between memory-driven exploitation and memory-free exploration, potentially leading to more efficient search behavior. This suggests that memory should be explicitly considered when designing efficient resetting protocols in viscoelastic or otherwise structured environments.

Data availability statement

All data that support the findings of this study are included within the article (and any supplementary files).

Supplemental material available at https://doi.org/10.1088/1367-2630/ae2dfc/data1

Acknowledgment

This work has been financially supported by the ERC Adv. Grant BRONEB (101141477).

ORCID iDs

Félix Ginot 0000-0001-9585-8613
Clemens Bechinger 0000-0002-5496-5268

References

[1] Bénichou O, Loverdo C, Moreau M and Voituriez R 2011 *Rev. Mod. Phys.* **83** 81–129
[2] Boyer D and Solis-Salas C 2014 *Phys. Rev. Lett.* **112** 240601
[3] Roldán E, Lisica A, Sánchez-Taltavull D and Grill S W 2016 *Phys. Rev. E* **93** 062411
[4] Bressloff P C 2020 *J. Phys. A: Math. Theor.* **53** 355001
[5] Evans M R and Majumdar S N 2011 *Phys. Rev. Lett.* **106** 160601
[6] Rotbart T, Reuveni S and Urbakh M 2015 *Phys. Rev. E* **92** 060101
[7] Fuchs J, Goldt S and Seifert U 2016 *Europhys. Lett.* **113** 60009
[8] Montero M, Masó-Puigdellosas A and Villarroel J 2017 *Eur. Phys. J. B* **90** 1–10
[9] Evans M R, Majumdar S N and Schehr G 2020 *J. Phys. A: Math. Theor.* **53** 193001
[10] Gupta S and Jayannavar A M 2022 *Front. Phys.* **10** 789097
[11] Lomholt M A, Tal K, Metzler R and Joseph K 2008 *Proc. Natl Acad. Sci.* **105** 11055–9
[12] Pal A and Reuveni S 2017 *Phys. Rev. Lett.* **118** 030603
[13] Chechkin A and Sokolov I M 2018 *Phys. Rev. Lett.* **121** 050601
[14] Besga B, Bovon A, Petrosyan A, Majumdar S N and Ciliberto S 2020 *Phys. Rev. Res.* **2** 032029
[15] Riascos A P, Boyer D, Herringer P and Mateos J L 2020 *Phys. Rev. E* **101** 062147
[16] Stanislavsky A and Weron A 2021 *Phys. Rev. E* **104** 014125
[17] Chen Y, Yuan Z, Gao L and Peng J 2023 *Phys. Rev. E* **108** 064109

[18] Chełminiak P, Wójcik J and Wójcik A 2025 *Phys. Rev. E* **111** 044143
[19] Avrachenkov K, Piunovskiy A and Zhang Y 2018 *Methodol. Comput. Appl. Probab.* **20** 1173–88
[20] Blumer O, Reuveni S and Hirshberg B 2022 *J. Phys. Chem. Lett.* **13** 11230–6
[21] Blumer O, Reuveni S and Hirshberg B 2024 *Nat. Commun.* **15** 240
[22] Boyer D, Evans M R and Majumdar S N 2017 *J. Stat. Mech.* 023208
[23] Bodrova A S, Chechkin A V and Sokolov I M 2019 *Phys. Rev. E* **100** 012119
[24] Gupta D 2019 *J. Stat. Mech.* 033212
[25] Wang W, Cherstvy A G, Kantz H, Metzler R and Sokolov I M 2021 *Phys. Rev. E* **104** 024105
[26] Singh P and Pal A 2021 *Phys. Rev. E* **103** 052119
[27] Chełminiak P 2022 *J. Phys. A: Math. Theor.* **55** 384004
[28] Colombani G, Bertagnolli G and Artime O 2023 *J. Phys. Complex.* **4** 04LT01
[29] Goswami K 2025 *Phys. Rev. E* **111** 014150
[30] Michelitsch T M, D'onofrio G, Polito F and Riascos A P 2025 *Chaos* **35** 013119
[31] Taźbierski K, Metzler R and Magdziarz M 2025 *New J. Phys.* **27** 074603
[32] Tal-Friedman O, Pal A, Sekhon A, Reuveni S and Roichman Y 2020 *J. Phys. Chem. Lett.* **11** 7350–5
[33] Goerlich R, Li M, Pires L B, Hervieux P A, Manfredi G and Genet C 2023 arXiv:2306.09503
[34] Bénichou O, Coppey M, Moreau M, Suet P and Voituriez R 2005 *Phys. Rev. Lett.* **94** 198101
[35] Bell W J 2012 *Searching Behaviour: the Behavioural Ecology of Finding Resources* (Springer Science & Business Media)
[36] Metzler R, Jeon J H, Cherstvy A G and Barkai E 2014 *Phys. Chem. Chem. Phys.* **16** 24128–64
[37] Falcón-Cortés A, Boyer D, Giuggioli L and Majumdar S N 2017 *Phys. Rev. Lett.* **119** 140603
[38] Altshuler A, Bonomo O L, Gorohovsky N, Marchini S, Rosen E, Tal-Friedman O, Reuveni S and Roichman Y 2024 *Phys. Rev. Res.* **6** 023255
[39] Cates M and Candau S 1990 *J. Phys.: Condens. Matter* **2** 6869
[40] Buchanan M, Atakhorrami M, Palierne J, MacKintosh F and Schmidt C 2005 *Phys. Rev. E* **72** 011504
[41] Ginot F, Caspers J, Reinalter L F, Kumar K K, Krüger M and Bechinger C 2022 *New J. Phys.* **24** 123013
[42] Khan M, Regan K and Robertson-Anderson R M 2019 *Phys. Rev. Lett.* **123** 038001
[43] Gupta S, Majumdar S N and Schehr G 2014 *Phys. Rev. Lett.* **112** 220601
[44] Gupta D, Plata C A, Kundu A and Pal A 2020 *J. Phys. A: Math. Theor.* **54** 025003
[45] Caspers J, Ditz N, Krishna Kumar K, Ginot F, Bechinger C, Fuchs M and Krüger M 2023 *J. Chem. Phys.* **158** 024901
[46] Sokolov I M 2023 *Phys. Rev. Lett.* **130** 067101
[47] Barkai E, Flaquer-Galmes R and Méndez V 2023 *Phys. Rev. E* **108** 064102
[48] Pal P S, Pal A, Park H and Lee J S 2023 *Phys. Rev. E* **108** 044117